Modification and Minimization of Spinel(Al$_2$O$_3$·xMgO) Inclusions Formed in Ti-Added Steel Melts

CHANG-WOO SEO, SEON-HYO KIM, SUNG-KOO JO, MIN-OH SUK, and SUN-MIN BYUN

High-melting-point inclusions such as spinel(Al$_2$O$_3$·xMgO) are known to promote clogging of the submerged entry nozzle (SEN) in a continuous caster mold. In particular, Ti-alloyed steels can have severe nozzle clogging problems, which are detrimental to the slab surface quality. In this work, the thermodynamic role of Ti in steels and the effect of Ca and Ti addition to the molten austenitic stainless steel deoxidized with Al on the formation of Al$_2$O$_3$·xMgO spinel inclusions were investigated. The sequence of Ca and Ti additions after Al deoxidation was also investigated. The inclusion chemistry and morphology according to the order of Ca and Ti are discussed from the standpoint of spinel formation. The thermodynamic interaction parameter of Mg with respect to the Ti alloying element was determined. The element of Ti in steels could contribute to enhancing the spinel formation, because Ti accelerates Mg dissolution from the MgO containing refractory walls or slags because of its high thermodynamic affinity for Mg ($e_{Mg}^{Ti} = -0.933$). Even though Ti also induces Ca dissolution from the CaO-containing refractory walls or slags because of its thermodynamic affinity for Ca ($e_{Ca}^{Ti} = -0.119$), dissolved Ca plays a role in favoring the formation of calcium aluminate inclusions, which are more stable thermodynamically in an Al-deoxidized steel. The inclusion content of steel samples was analyzed to improve the understanding of fundamentals of Al$_2$O$_3$·xMgO spinel inclusion formation. The optimum processing conditions for Ca treatment and Ti addition in austenitic stainless steel melts to achieve the minimized spinel formation and the maximized Ti-alloying yield is discussed.

I. INTRODUCTION

IN the pursuit of better cleanliness of the strip surface, improved steelmaking practices to control the quantity and composition of inclusions in steel are required. The existence of hard inclusion such as spinel deteriorates the final quality of steel products because it has a high melting point and exists as a C-type inclusion,[1] which is not plastically deformed and not evenly dispersed. It also induces the submerged entry nozzle clogging of a continuous casting process, which decreases productivity yield and slab surface quality. Therefore, a means of preventing and minimizing the occurrence of spinel formation in a given steel composition is requisite for the production of high-grade clean steels.

Some studies to clarify the formation mechanism of spinel inclusion have been reported. Itoh et al.[2] studied the inclusion compositions in liquid steel deoxidized by Al in a dolomite crucible. The experimental results agree with the phase stability diagram of spinel inclusion estimated from the existing thermodynamic data. Ohta and Suito[3] studied the thermodynamic equilibria of Ca-O and Mg-O in liquid iron with CaO-SiO$_2$-Al$_2$O$_3$-MgO slags on top at 1873 K (1600 °C) using a CaO or MgO crucibles. In their report, the phase stability regions in Fe-Al-Ca-O and Fe-Al-Mg-O systems at 1873 K (1600 °C) are in reasonable agreement with the experimental data. Some works performed by Nishi and Shinme[4] and Okuyama et al.[5] focused on the effect of slag basicity on MgO content in inclusions in a stainless steel. Kim et al.[6] reported that the spinel inclusion in the type 304 stainless steel melt deoxidized by Al and Ti could be avoided by decreasing both MgO content in an argon oxygen decarburization (AOD) slag and Al content in the melt. These previous investigations[2–5] indicated that the presence of a limited amount of dissolved Mg and Al (a couple of mass ppm) enables the formation of spinel inclusion in steels.

The attractive interaction between the added Ti in steels and the dissolved Mg from the slag or refractory could explain the frequent detection of spinel inclusion in Ti added austenitic stainless steel deoxidized with Al. However, only a few available reports[7–11] have discussed the experimental determination of the interaction parameters between Mg and other elements dissolved in liquid iron, as shown in Table I. To ascertain the role of

CHANG-WOO SEO, Graduate Student, and SEON-HYO KIM, Professor, are with the Department of Materials Science and Engineering, Pohang University of Science and Technology, Pohang 790-784, Korea. Contact e-mail: seonhyo@postech.ac.kr SUNG-KOO JO, Researcher, is with the Research Institute of Industrial Science & Technology, Pohang 790-600, Korea. MIN-OH SUK, Researcher, and SUN-MIN BYUN, Principal Researcher, are with the Stainless Steel Research Group, Technical Research Laboratories, POSCO, Pohang 790-785, Korea.
Manuscript submitted April 23, 2009.
Article published online May 11, 2010.

the dissolved Ti regarding spinel formation, the equilibria between Mg vapor and third elements in liquid iron were investigated by Han[10] and Jo et al.[11] with employing a sophisticated experimental apparatus. In these studies, the volatile vapor/liquid equilibration method[12] was applied to determine quantitatively the effect of a third element Ti on the behavior of Mg activity in liquid iron at 1873 K (1600 °C). However, Han[10] did not consider the effect of oxygen on Mg behavior, viz. the interaction parameters between Mg and oxygen. Thus, the oxygen effect was taken into account using the reported values on e_{Mg}^O, r_{Mg}^O, and $r_{Mg}^{Mg,O}$[12] by Jo et al.[11] The results were discussed in regard to the thermodynamic potential of Ti to cause the element of Mg dissolution into steel from slag or refractory materials and, finally, to facilitate the formation of spinel in steel.

Considering the effect of Ti on Ca behavior, few studies have examined the interaction parameter between Ti and Ca, including Song and Han[16] in Table I. But, as in earlier studies that involved Mg,[10] the previous work did not consider the effect of oxygen on Ca behavior, which is too significant to be neglected.

Therefore, in the current experiments, the samples were prepared using the vacuum arc melting (VAM) method, and their soluble oxygen contents were below 10 mass ppm. Additionally, multiple experiments were conducted at the same liquid Mg or Ca temperatures to assess the reliability and reproducibility of the data.

Calcium treatment[17,18] is a countermeasure to avoid harmful alumina or spinel inclusions by modifying them to harmless liquid calcium aluminate inclusions. Calcium modification of Ti-bearing inclusions in steel contributes to the production of high-quality steel with fewer defects caused by inclusions,[19] and it prevents nozzle blockage by inclusion buildup during casting. Because under normal steelmaking conditions, calcium aluminates are favored to form thermodynamically compared with spinel inclusions. The dissolved Ca can reduce spinel inclusions and convert them into calcium aluminates.[20–22] From previous papers,[2–5] the reaction of spinel formation takes place when only a few mass ppm of dissolved Mg is present in liquid steel. Considering the effect of dissolved Ca in steel, the stable region of spinel phase was moved to greater contents of dissolved Mg and Al. And in the study by Higuchi

et al.,[23] dissolved calcium in melt reacts rapidly with alumina inclusions to form calcium aluminate. However, in comparing the formation of calcium aluminate and that of spinel, the formation of spinel occurs continuously because of a steady supply of Mg from the reduction of MgO contained in slags or refractories. Thus, it is of interest to explore the effect of changing sequential orders between Ti alloying and Ca treatment after Al deoxidation.

In the previous articles, the effect of Ca and Ti addition sequence on the inclusion behavior and relevant steel cleanness was not considered. Therefore, in this work, for the prevention and modification of these deleterious spinel inclusions, the effect of changing the order of Ca treatment and Ti addition has been investigated. The inclusion chemistry and morphology according to those sequential orders will be discussed from the standpoint of spinel formation and its mechanism.

II. EXPERIMENTAL

An equilibrium study between Mg or Ca vapor and liquid iron was carried out 1873 K (1600 °C) in a LaCrO$_3$ resistance furnace with a fused alumina tube of 70 mm diameter and hot zone length of 5 mm. A molybdenum reaction chamber sealed with an iron lid was installed inside the tube. A schematic diagram of the experimental apparatus is shown elsewhere in detail.[24] The seven MgO crucibles containing 10 g of an appropriate amount of Fe-Ti alloy made by VAM were positioned in the hot temperature zone (1873 K (1600 °C)) of a Mo chamber where the reaction temperature was controlled within an accuracy of ±2 K (2 °C). Another MgO crucible containing Mg granules (99.9 pct) or Ca granules (99.5 pct) was then placed on the Mo wire mesh between the Fe lid and Mo chamber, where the temperature is maintained from 923 K (650 °C) to 1500 K (1227 °C) according to the height of the Fe lid. The Mo chamber sealed by the Fe lid was initially under an Ar atmosphere where any residual oxygen could react quickly with Mg or Ca vapor, and its product is deposited on the wall of the Fe lid. The liquid Mg temperature (T_{Mg}) or Ca temperature (T_{Ca}) was measured by a Ni/Cr10-Ni/Al3/Si3 thermocouple

Table I.   Summary of Previously Available Values of e_{Mg}^i and e_{Ca}^i in Liquid Iron at 1873 K (1600 °C)

Authors	e_{Mg}^{Al}	e_{Mg}^{Cr}	e_{Mg}^{Ni}	e_{Mg}^{Ti}	e_{Mg}^{Si}	e_{Mg}^{C}
Sigworth and Elliott[7]	—	—	—	—	—	0.14
Nadif and Gatellier[8]	—	0.01	−0.012	—	—	—
Turkdogan[9]	—	—	—	—	−0.046	−0.15
Han[10]	−0.12	0.05	−0.03	−0.51	−0.09	−0.25
Jo et al.[11]	−0.277	0.022	−0.033	−0.64	−0.096	−0.31

Authors	e_{Ca}^{Al}	e_{Ca}^{Cr}	e_{Ca}^{Ni}	e_{Ca}^{Ti}	e_{Ca}^{Si}	e_{Ca}^{C}
Nadif and Gatellier[8]	—	—	−0.049	—	—	—
Ageev and Archugov[13]	—	—	−0.03	—	−0.074	—
Sponseller and Flinn[14]	−0.072	—	−0.044	—	−0.097	−0.337
Kohler et al.[15]	−0.054	0.014	−0.043	—	−0.096	—
Song and Han[16]	—	−0.18	−0.097	−0.13	−0.11	—

embedded inside the iron lid. After reaching the desired reaction temperature, the molybdenum chamber was tightly sealed by an iron lid because of the difference of thermal expansion coefficients between Mo and Fe. After holding the reaction for 5 hours, which is sufficient for achieving the equilibrium state as confirmed in the previous work,[24,25] the molybdenum chamber sealed with a Fe lid was taken out of the furnace. The Mo chamber part was quenched rapidly in ice water to prevent Mg or Ca evolution from the Fe-Ti melt during quenching, whereas the Fe lid was quenched slowly in air.

To investigate the effect of dissolved Mg or Ca from the CaO-MgO refractory and the alloyed Ti elements on inclusion chemistry and morphology, 400 g AOD steel (0.04 pct C, 0.6 pct Si, 1.4 pct Mn, 16.8 pct Cr, 10.7 pct Ni, and 2.1 pct Mo) and 20 g CaCO$_3$-MgCO$_3$ mixture (50:50 weight ratio) plate simulating the refractory were placed inside a MgO crucible (OD: 45 mm, ID: 40 mm, and H: 150 mm) housed by a 15 kW/50 kHz high-frequency induction furnace where the temperature was increased to 1873 K (1600 °C) (Figure 1). The CaCO$_3$-MgCO$_3$ mixtures could transform into CaO-MgO compound by complete calcination at 1873 K (1600 °C). The temperature of the crucible in contact with the melt was measured with a thermocouple of Pt/6 pct Rh-Pt/30 pct Rh. The thermocouple was connected to the proportional–integral–derivative controller of the induction furnace, which automatically adjusted the induction power to maintain steel melt temperature of 1873 K ± 10 K (1600 °C ± 10 °C). After reaching the desired temperature, the appropriate amounts of Al (99.99 pct), Ti (99.99 pct), and Ca (99.5 pct) granules, which were wrapped in Fe foil and kept initially in a quartz tube by magnet, were dropped into the melt. The steel samples were taken at 5, 18, and 25 minutes (corresponding to 5 minutes after Al deoxidation, Ti alloying, and Ca treatment, respectively), and finally at 55 minutes.

Quenched samples from both experiments were sliced into thin sections and then divided into smaller pieces for chemical and inclusion analyses. The Ca, Mg, and other elements were measured by the inductively coupled plasma emission spectrometry. The oxygen was analyzed by the inert-gas fusion infrared absorptiometry. The morphology of inclusions was observed using a scanning electron microscope and their compositions were determined by energy-dispersive spectrometry.

III. RESULTS AND DISCUSSION

The experimental data on the equilibrium study to investigate the effect of Ti on the dissolved amount of Mg or Ca in liquid iron at 1873 K (1600 °C) are listed in Table II. The temperature of liquid Mg or Ca (T$_{Mg}$ or T$_{Ca}$), during the experiment, is also shown in Table II.

The temperature dependence of the saturated vapor pressures of Mg or Ca are represented, respectively,[25,26]

$$logP_{Mg} = 9.91 - 1.41logT_{Mg} - 7750/T_{Mg}^{[25]} \quad [1]$$

$$logP_{Ca} = 5.46 - 9670/T_{Ca}^{[26]} \quad [2]$$

where the unit of P$_{Mg}$ and P$_{Ca}$ is in atm and temperature is in Kelvin. First, the dissolved content Mg in the binary Fe-Mg and the ternary Fe-Ti-Mg solutions under the identical P$_{Mg}$ condition in the Mo chamber were determined. Because the binary and ternary iron melts are saturated with Mg under the same P$_{Mg}$ and temperature, the following equilibrium condition is satisfied:

$$f'_{Mg}[pct\ Mg]' = f_{Mg}[pct\ Mg] \quad [3]$$

where, f'_{Mg} and f_{Mg} are the activity coefficients of Mg with respect to the 1 mass pct standard state for the Fe-Mg and Fe-Mg-Ti solutions, respectively. [pct Mg]'

Fig. 1—Schematic diagram of experimental induction furnace.

Table II. Composition of Metal Samples and Equilibrated with Mg or Ca Vapors of 1873 K (1600 °C)

Fe-Mg-Ti system (T$_{Mg}$ = 1059 K (786 °C))		
[mass pct Ti]	[mass pct Mg]	−log[mass pct Mg]
0.2110	0.0026	2.5850
0.4564	0.0049	2.3098
0.6734	0.0058	2.2366
0.8121	0.0096	2.0177
1.0034	0.0183	1.7375
1.2343	0.0267	1.5735
1.5323	0.0395	1.4034

Fe-Ca-Ti system (T$_{Ca}$ = 1438 K (1165 °C))		
[mass pct Ti]	[mass pct Ca]	−log[mass pct Ca]
0.2138	0.0027	2.5686
0.4243	0.0029	2.5376
0.7932	0.0032	2.4915
0.9873	0.0034	2.4737
1.2342	0.0036	2.4437
1.9811	0.0043	2.3665
2.2131	0.0046	2.3372

and [pct Mg] are the saturated dissolved contents of Mg in Fe-Mg binary and the Fe-Mg-Ti ternary melts, respectively.

$$f_{Mg}^i = f_{Mg}/f'_{Mg} = [pct\ Mg]'/[pct\ Mg] \qquad [4]$$

According to the definition of interaction parameter,

$$\lim_{[pct\ i]\to 0}\left(\partial \log f_{Mg}^i \Big/ \partial \log[pct\ i]\right)_{a'_{Mg}=a_{Mg}} = e_{Mg}^{*i}$$

$$e_{Mg}^{*i} = \lim_{[pct\ i]\to 0}(\partial \log[pct\ Mg]/\partial[pct\ i])_{a'_{Mg}=a_{Mg}} \qquad [5]$$

By plotting $-\log[pct\ Mg]$ against [pct Ti] in Table II and applying a linear regression in equation form of $-\log[pct\ Mg] = A + e_{Mg}^{*Ti}$ [pct Ti], the value of e_{Mg}^{*Ti} could be determined from the slope. Using the relationship $e_{Mg\ or\ Ca}^{Ti} = e_{Mg\ or\ Ca}^{*Ti}$ $(1 + 2.30[pct\ Mg\ or\ Ca]'\ e_{Mg}^{Mg}$ or $e_{Ca}^{Ca})$,[27] the values of e_{Mg}^{Ti} and e_{Ca}^{Ti} could be evaluated. However, because of the low concentration of Mg and Ca, their effects on the measured interaction parameter can be neglected. And thus, the values of e_{Mg}^{Ti} and e_{Ca}^{Ti} are equal to those of e_{Mg}^{*Ti} and e_{Ca}^{*Ti}. The values of e_{Mg}^{Ti} and e_{Ca}^{Ti} are determined as -0.933 and -0.119, respectively, from the present regression in Figure 2. The negatively large value of e_{Mg}^{Ti} indicates that Ti has a thermodynamic potential to decrease the activity coefficient of Mg in liquid iron. Such an element could accelerate the elemental Mg dissolution into molten steels from slag or MgO-bearing refractory materials and could play a role in favoring the formation of spinel inclusions in an Al deoxidized steel. Therefore, Ti is considered to be a significantly influential element in spinel formation for the case of steel grades that contain large amounts of Ti such as on 321 austenitic stainless steel (Ti > 0.25−0.3 mass pct), because the magnitude of e_{Mg}^{Ti} is negatively large (-0.933). A similar result was reported in the previous work,[28] which investigated the composition and morphology changes of deoxidation products in the slag/metal (Fe-16 mass pct Cr)/MgO crucible system.
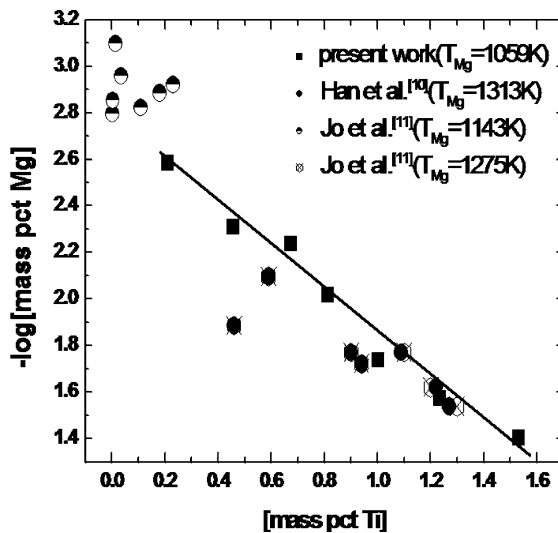
Figure 3 shows the types of inclusions in Cr containing steels for the cases of Si-Al and Si-Al-Ti deoxidation, which were observed with the help of scanning electron microscopy.[28] In the case of Ti addition (0.0053 mass pct Ti), the initially formed FeO-Al_2O_3 inclusions are transformed into Al_2O_3-SiO_2 and subsequently to spinel, whereas Al_2O_3-SiO_2 remained as a stable inclusion for Si-Al deoxidation. Therefore, Ti should be added with careful attention to avoid spinel formation for the production of high-grade clean steels.

Similar to the Fe-Ti-Mg ternary system, the value of e_{Ca}^{Ti} can be determined from the regression line for Fe-Ti-Ca system as shown in Figure 2. The negative value of e_{Ca}^{Ti} indicates that Ti has a thermodynamic potential to decrease the activity coefficient of Ca in liquid iron. Such an element could enhance the elemental Ca dissolution into molten steels very locally from slag or CaO-bearing refractory materials, only if the Ti level is relatively high. This dissolved Ca plays a role in favoring the formation of calcium aluminate inclusions.

The conventional ladle-refining process for the production of austenitic stainless steel 321 grade is composed of the following sequential treatments. The liquid
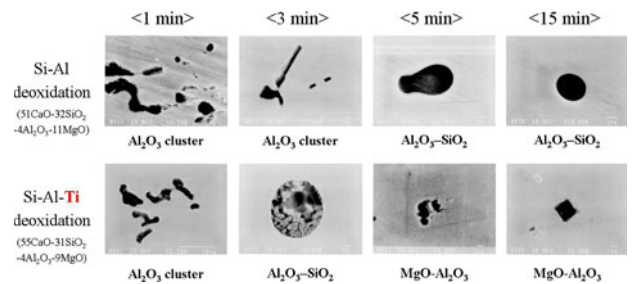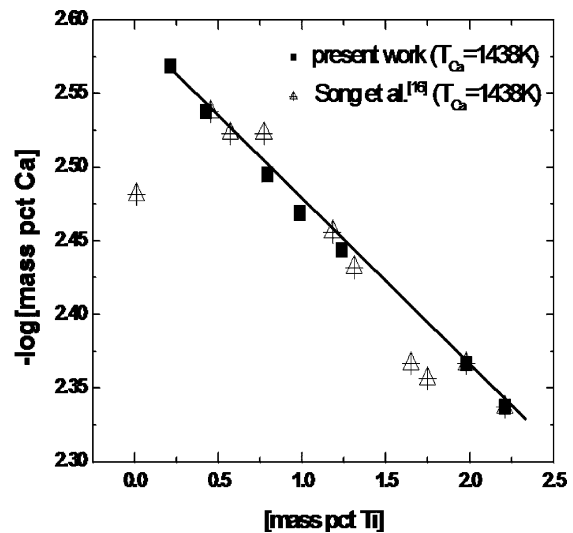

Fig. 3—Variations of inclusion composition according to processing times after deoxidation of Fe-16 mass pct Cr by Si-Al (a) and Si-Al-Ti (b).[28]

Fig. 2—Regression lines according to Eq. [5] for Fe-Ti-Mg (or Ca) system.

steel is deoxidized initially with Al and then Ti is added for compositional control of about 0.05 mass pct Al and 0.3 mass pct Ti. Thereafter, for the modification of inclusions such as alumina and spinel, the steel is treated by Ca addition (referred to as the "ATC" practice). From the previously mentioned thermodynamic assessment, it is known that adding Ti as an alloying element could accelerate Mg dissolution into molten steels from slag or MgO-bearing refractory materials. The dissolved Mg into the Al-killed steels combines with Al_2O_3 to form $Al_2O_3 \cdot xMgO$ spinel inclusions. Therefore, to reduce the formation of spinel inclusions, it may be advantageous to conduct Ca treatment prior to Ti alloying (referred to the "ACT" practice).

In the current work, the effect of changing the sequence of Ti addition and Ca treatment on the spinel formation was examined kinetically. The experimental results that show the variations of Ca, Mg, and total oxygen in steel according to time from beginning of experiment are represented in Figure 4. Similar to the effect of Ti on dissolved Mg in steel, the attractive interaction between dissolved Al and Mg ($e_{Mg}^{Al} = -0.12$[10] or -0.277[11] in Table I) in steel indicates that Al has a thermodynamic potential to decrease the activity coefficient of Mg in liquid iron. Thus, Al could induce the Mg dissolution into molten steels from slag or MgO-bearing refractory materials. Therefore, the Mg content increases right after the Al deoxidation, and this tendency was identical in both ATC and the ACT practice. Mg content also increases by the following Ti addition for the ATC practice. The Ca content in steel is also increased by the following Ca treatment.

In the ACT procedure, the increase of Ca content is more significant and results in lower total oxygen content. Ca is supposed to be dissolved more effectively for the ACT procedure, and as a result, the dissolved Ca tends to react with alumina inclusions to form the inclusions of lower melting temperature. In view of oxygen potential, the Ca treatment before the Ti addition procedure could contribute to decreasing the oxygen potential more effectively than the *vice versa*

procedure. The lower oxygen potential enables more effective Ti dissolution for the ACT procedure, and as a result, the more dissolved quantity of Ca tends to react with alumina inclusions. In the ATC practice, the total oxygen content was nearly constant as 20 mass ppm during the entire experiment. The oxygen content was finally decreased to 10 mass ppm after Ca treatment in the ACT practice, as shown in Figure 4.

In Figure 5, the variations of inclusion composition are compared for a sample of 100 inclusions from both the ATC and ACT test practices. Before Al deoxidation, Al_2O_3-SiO_2 and slag type inclusions, such as CaO-Al_2O_3-SiO_2-MgO, existed. These inclusions are from AOD slags whose compositions are CaO-SiO_2-Al_2O_3-MgO. The deoxidation of the initial melts by Al forms alumina and spinel type ($Al_2O_3 \cdot xMgO$) inclusions. Thereafter, TiO_2 containing inclusions and additional spinel were formed by Ti addition in the ATC practice. A limited quantity of CaO-Al_2O_3 inclusions was formed by the following Ca treatment, because of the depletion of available Al_2O_3 by Ti addition in advance. Spinel type inclusions were still found in the samples taken after Ca treatment. Moreover, deleterious inclusions such as TiO_2 or Al_2O_3-TiO_2 remained. The modification of Al_2O_3 inclusions is not effective. Furthermore, the addition of Ca could form some CaO·TiO_2 inclusions.

For the ACT practice, the alumina inclusions are modified to calcium aluminate inclusions by the reaction with dissolved Ca, which is supplied from the Ca treatment before Ti addition. The CaO-Al_2O_3 inclusions do not change to spinel even after the subsequent Ti addition because Al_2O_3 in the CaO-Al_2O_3 inclusions does not react easily with MgO because of the reduced activity of Al_2O_3. The contents of TiO_2 in the ACT practice were also low in comparison with those in the ATC practice, because dissolved Ca reacts with oxygen effectively and decreases the oxygen potential in steel.

From Figures 6 and 7, the typical variations of inclusion morphology are shown. For both practices (ATC and ACT), alumina inclusions show a cluster morphology. For the ATC practice, typical
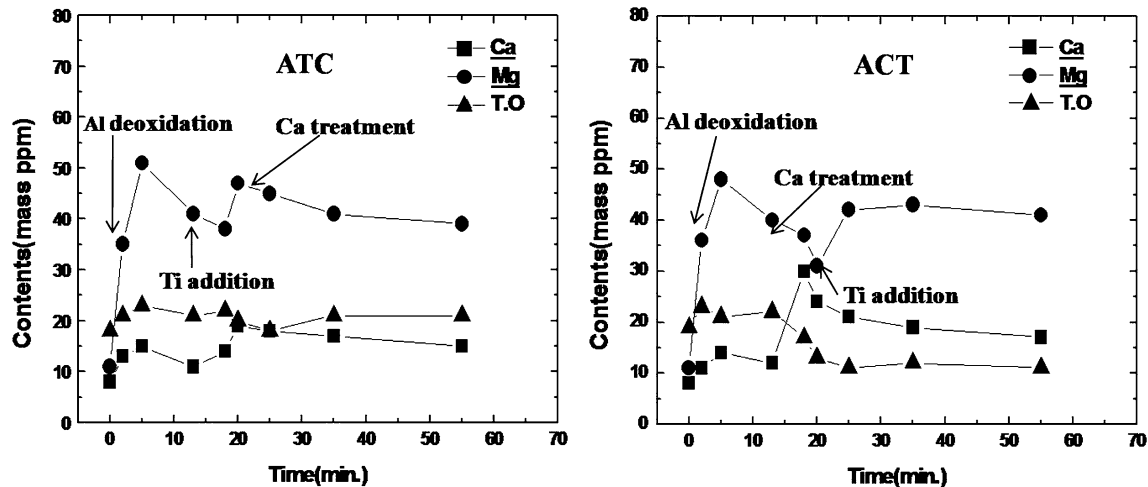

Fig. 4—Variations of Ca, Mg, and total oxygen in steel as a function of processing time for ATC and ACT practices.

Fig. 6—Compositional and morphological variations of inclusion observed in a steel melt treated by the ATC practice.

Fig. 7—Compositional and morphological variations of inclusion observed in a steel melt treated by the ACT practice.
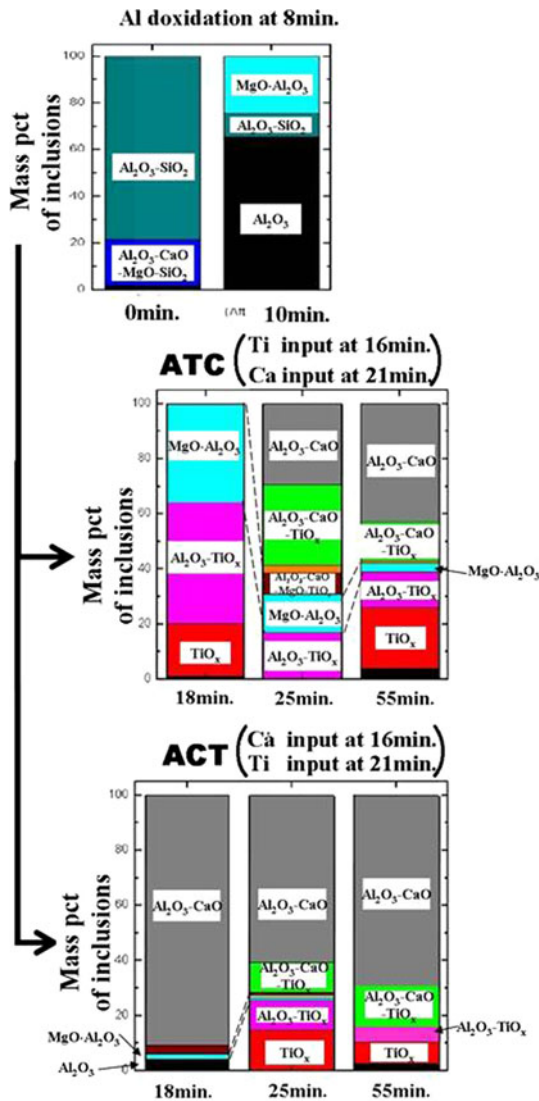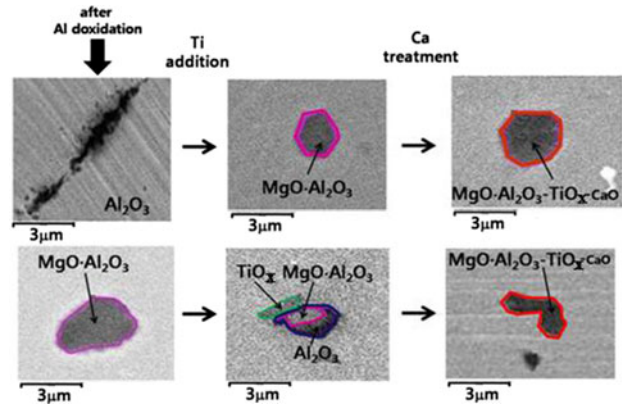
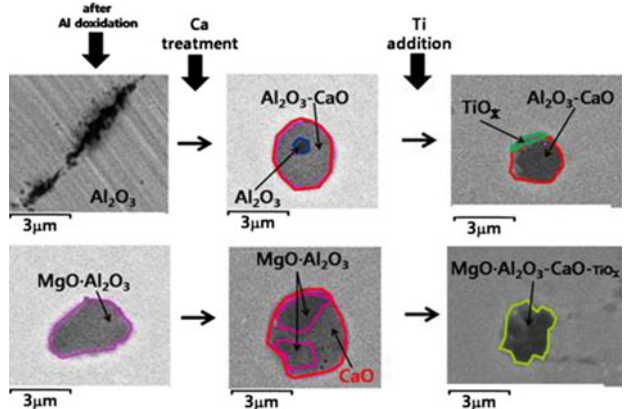Fig. 5—Variation of inclusion compositions in an AOD steel melt as a function of processing times coupled with additions of various additives employing the experimental apparatus in Fig. 1.

angular-shaped spinel inclusions appear after Ti alloying. Moreover formed spinel inclusions by Al deoxidation are not only remained but also complicated with Al_2O_3-TiO_2 inclusions. Thereafter, even though Ca treatment is conducted, the morphology of the spinel inclusions is not effectively modified, whereas for the ACT practice, Al_2O_3 inclusions transform into calcium aluminate inclusions easily. Spinel inclusions are surrounded by globular calcium aluminate after Ca treatment. Figure 8 shows the compositional variation of various inclusions with respect to the treating time in a ternary diagram. For both practices, Al_2O_3 and spinel inclusions tend to form after Al deoxidation. For the ATC practice, the MgO content in Al_2O_3 inclusions is increased by the Ti addition, which also induces TiO_x formation. Thereafter, the limited quantities of CaO combined with Al_2O_3 inclusions result from Ca treatment. However for the ACT practice, Al_2O_3 inclusions

are actively modified to calcium aluminates. Subsequently, the less TiO_x-containing inclusions were formed by Ti addition in comparison with the ATC practice.

In the current work, the activity of alumina can be approximated as one because Al deoxidation occurred without a slag phase present. As mentioned previously, the Mg contents near the refractory wall significantly increase by soluble Ti and Al in terms of e_{Mg}^{Ti}, e_{Mg}^{Al}. The dissolved Mg reacts with Al_2O_3 inclusions to form spinel inclusions. Its reaction rate seems slow but spinel is formed continuously

However, the ACT practice forms calcium aluminate with a low melting point. That is, the most alumina inclusions whose activity of Al_2O_3 is nearly one are modified to calcium aluminate inclusions by reaction with Ca. Thus, only the limited quantities of Al_2O_3 are available for the formation of spinel even after subsequent Ti addition. Actually, the spinel inclusions in the austenitic stainless steel samples obtained from the plant operation could be detected only 5 minutes after the Ti addition, which indicates the formation rate of spinel between Al_2O_3 and the dissolved Mg from the refractory or slag seems to be slow. Thus, the earlier Ca addition after Ti addition helps to reduce the potential for spinel formation than *vice versa*.
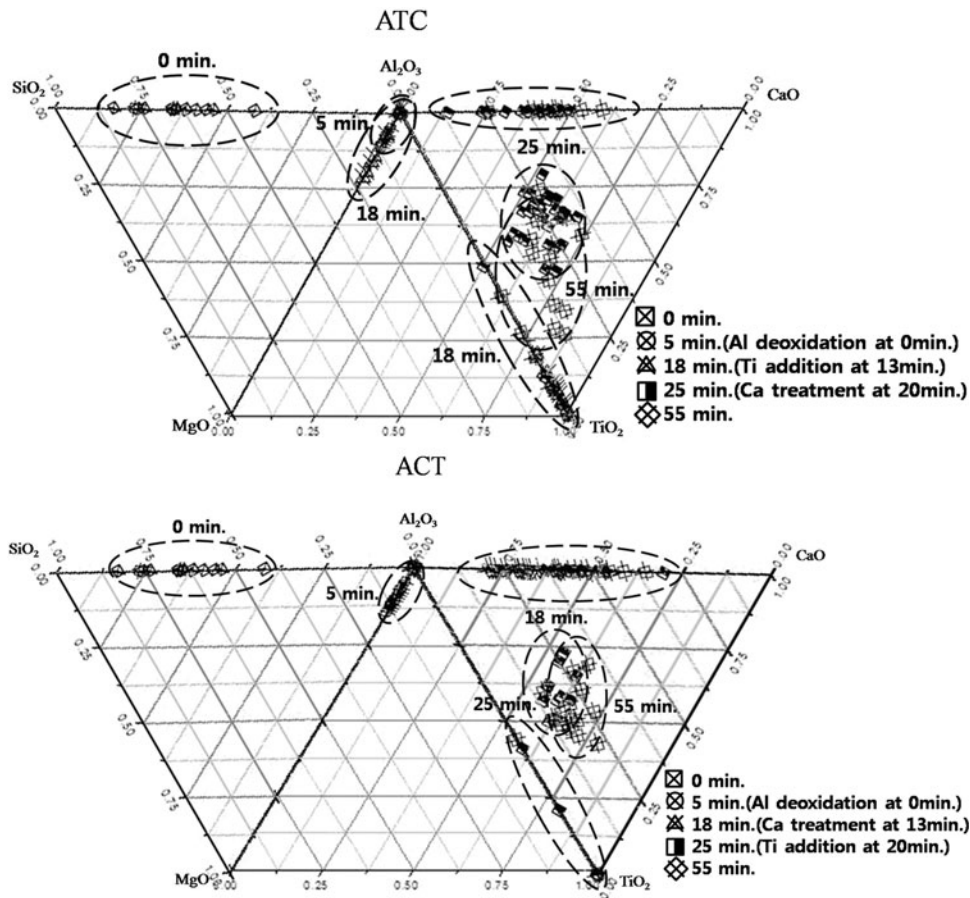
Fig. 8—Change of inclusion compositions as a function of time between the ATC and ACT practices.

IV. CONCLUSIONS

For the modification and prevention of inclusions, the effect of sequential orders of charging alloying element Ti and Ca treatment was assessed thermodynamically and kinetically. To clarify the thermodynamic role of Ti in steels, the interaction parameters between Mg (or Ca) and Ti were determined using the vapor/liquid equilibration method at 1873 K (1600 °C). The interaction parameters of Mg and Ca with respect to Ti at 1873 K (1600 °C) determined in this work are as follows:

$$e_{Mg}^{Ti} = -0.933, \ e_{Ca}^{Ti} = -0.119$$

The Ca treatment after Ti addition (ATC) is not an effective way to minimize the spinel formation, because Ti could accelerate the reduction of Mg from the MgO-containing refractory wall or slag because of its high thermodynamic affinity for Mg in iron. After the initial Al deoxidation, the following Ti addition helps the acceleration of Mg reduction from MgO refractory into molten steels so that spinel inclusion is formed easily and builds up.

The ACT practice efficiently prevents the formation of spinel followed by Ti addition because of the depletion of available Al_2O_3 by the earlier Ca operation. The formation reaction of spinel inclusions could be suppressed, and even a few spinel inclusions formed are mostly modified into the globular shape enclosed by calcium aluminates.

Consequently, the ACT pattern of the ladle refining operation could reduce the spinel formation successfully in Ti-alloyed steels and could extend the life cycle of SEN nozzle.

REFERENCES

1. Japanese Standards Association: *JIS Handbook*, Japanese Standards Association, Tokyo, Japan, 2001, vol. 1, p. 404.

2. H. Itoh, M. Hino, and S. Ban-ya: *Tetsu-to-Hagane*, 1998, vol. 84, pp. 90–98.
3. H. Ohta and H. Suito: *Metall.Mater. Trans. B*, 1997, vol. 28B, pp. 1131–39.
4. T. Nishi and K. Shinme: *Tetsu-to-Hagane*, 1998, vol. 84, pp. 837–43.
5. G. Okuyama, S. Takeuchi, and K. Sorimachi: *CAMP-ISIJ*, 1997, vol. 10, p. 847.
6. J.W. Kim, S.K. Kim, D.S. Kim, Y.D. Lee, and P.K. Yang: *Iron Steel Inst. Jpn. Int*., 1996, vol. 36, pp. S140–43.
7. G.K. Sigworth and J.F. Elliott: *Met. Sci.*, 1974, vol. 8, pp. 298–310.
8. M. Nadif and C. Gatellier: *Rev. Metall. CIT*, 1986, pp. 377–94.
9. E.T. Turkdogan: *Fundamentals of Steelmaking*, The Institute of Materials, London, UK, 1996, pp. 119–21.
10. Q. Han: *Proc. 6th Int. Iron and Steel Congr., ISIJ*, Nagoya, Japan, 1990, vol. 1, pp. 166–76.
11. S.J. Jo, B. Song, and S.H. Kim: *Metall. Mater. Trans. B*, 2002, vol. 33B, pp. 703–09.
12. J.D. Seo and S.H. Kim: *Steel Res.*, 2000, vol. 71, pp. 101–06.
13. Y.A. Ageev and S.A. Archugov: *J. Phys. Chem.*, 1985, vol. 59 (4), pp. 838–41 (in Russian).
14. D.L. Sponseller and R.A. Flinn: *Trans. TMS-AIME*, 1964, vol. 230, pp. 876–88.
15. M. Kohler, H.J. Engel, and D. Janke: *Steel Res.*, 1985, vol. 56, pp. 419–23.
16. B. Song and Q. Han: *Metall. Mater. Trans. B*, 1998, vol. 29B, pp. 415–20.
17. E.T. Turkdogan: *Fundamentals of Steelmaking*, The Institute of Materials, London, UK, 1996, pp. 285–94.
18. Y. Hayashi, M. Kanno, H. Yoshida, S. Inada, T. Kawahara, and S. One: *Proc. 6th Int. Iron and Steel Congr., ISIJ*, Nagoya, Japan, 1990, pp. 551–57.
19. H.S. Song, J.M. Lee, D.S. Lee, and E.S. Lee: Korean patent, KOR102003008884, 2005.
20. H. Todoroki and K. Mizuno: 2003, *Trans. ISS*, pp. 60–67.
21. K. Mizuno, H. Todoroki, M. Noda, and T. Tohge: 2001, *Trans. ISS*, pp. 93–101.
22. E.B. Pretorius: *AIST 2009 Proceedings*, pp. 1035.
23. Y. Higuchi, M. Numata, S. Fukagawa, and K. Shinme: *Iron Steel Inst. Jpn. Int*., 1996, vol. 36, pp. S151–54.
24. J.D. Seo and S.H. Kim: *Bull. Kor. Inst. Met. Mater*., 1999, vol. 12, pp. 402–10.
25. X. Zhang, Q. Han, and D. Chen: *Metall. Trans. B*, 1991, vol. 22B, pp. 918–21.
26. E. Rudberg: *Phys. Rev.*, 1934, vol. 18, p. 362.
27. T. Fuwa and J. Chipman: *Trans. AIME*, 1954, vol. 215, p. 708.
28. H.J. Jeong: Master's Thesis, Pohang University of Science and Technology, Pohang, Korea, 2001.